3D Lung Nodule Segmentation and ClassificationBased on Convolutional Neural Network Using V-Net Architecture

S. Lalitha[1], D. Murugan[2]

[1]*Research Scholar, Departmentof Computer Science and Engineering,ManonmaniamSundaranar University, Tirunelveli, India.*
[2]*Professor, Departmentof Computer Science and Engineering, ManonmaniamSundaranar University, Tirunelveli, India.*

[1]lalithasakthivelu73@gmail.com, [2]dhanushkodim@yahoo.com

Abstract *-Lung cancer is the leading cause of mortality worldwide. On an annual basis, lung cancer is responsible for more deaths than all other prevalent types of cancer combined. While there have been great strides made in the field of healthcare, this issue persists. Although most instances are discovered at stages 3 and 4, by which time it's much too late to treat successfully, early detection is key. The mortality rates associated with lung cancer are among the highest of any cancer kind. Consequently, early detection of lung nodules is crucial for improving survival rates. Some CAD systems can detect and categorize these nodules at an early stage. Data collecting, pre-processing, lung segments, nodule identification, false positive reductions, edge detection, and classifications are all now included in CAD systems for lung nodules. The purpose of this work is to develop an effective CAD system for segmenting a CT image of the lung, which will aid radiologists in the early detection and diagnosis of lung cancer. To improve nodule classification, a novel 3-D convolutional neural network (CNN) is employed to segment the CT image. Multiple enhancements were developed to guarantee lightning-fast communication and pinpoint precision in the final output. Specifically, the LUNA16 challenge's LIDC/IDRI database is performed to analyze the design. Our results show that deep learning with focused loss is a superior classification technique, with an accuracy of 97.10%, a sensitivity of 98.00%, and a precision of 97.93%.*

Keywords *-Computer Aided Diagnosis, Computer Tomography, 3D Convolutional Neural Network, Images Distributed Resource Initiative, Lung Images Dataset Cooperative*

1. Introduction

Lung cancer represents a serious threat to human health and life since that is one of the most lethal forms of cancer. The prevalence and mortality rate from lung cancer has greatly increased during the last half-century in several nations. To illustrate, the ACS estimates that there would be 1,898,160 new cancer deaths in 2021, with an estimated 608,570 deaths as a direct result of the disease. Lung nodules are often the first detectable evidence of lung disease on an x-ray. This is because lung nodules are the most accurate cancer in its early detection indicator. The risk posed by a nodule depends on its size. Nodules are typically small, round areas in the bronchospasm interstitial [1], which is a collection of assistance organs in the respiratory that also includes the soft tissue epithelium, the endothelium of small blood vessels, the basal lamina, and the connective tissue involving the ventricles and the perilymphatic spaces [2, 3]. Nodules in the lungs may vary from small to large and could be of varying ways [3]. Some nodules are spherical, with a diameter ranging from 2 mm to 30 mm [4]; both of these granulomas have convoluted vascular connections, making them more difficult to locate due to their proximity to major blood arteries. To provide just one piece of evidence, the incidence of solid nodules (SN) and sub-solid nodules (SSNs) is still only substantially stronger than that of the lung parenchyma surrounding them [5]. The most frequent type of nodule is the small pulmonary nodule (SNS), which is constituted of vital lung tissue. On the other hand, SSNs are a kind of lung tumor characterized by a low degree of ground-glass opacity (GGO). Completely solid nodules and ground-glass nodules are two distinct types of SSNs [6]. These nodules have higher based testing or structural testing levels than the surrounding structures, but they do not obscure the bronchovascular processes underneath [7]. Since the presence of cancer is correlated with the thickness of a nodule, accurate measurements of nodule surface area are crucial. There is a plethora of research [1,8,9] that provides advice on how to accomplish this goal. According tothe Fully completed Capacity as well as Consumer Evaluations Application (ELCAP) database [3], pituitary growths relatively small than 5 mm in diameter have a % malignant growth rate, erythematous between 6 mm and 10 mm have a 24 percent rate, nodules between 11 mm and 20 mm have a 33 percent rate, and nodules larger than 20 mm have an 80 percent rate of becoming malignant. However, inaccuracies

might be made when estimating the diameter of the tiny nodules see figure 1 below. Nodules in the lung cancer diagnosis are refractory to treatment because of their complexity. Radiation therapy is an essential aspect of treatment for over 70% of individuals with lung cancer. Light airway inflammation, however, is a known radiation treatment side effect that has been linked to a decreased rate of improvement and an increased risk of illness and death. When it concerns nodules, the radiologist may benefit significantly from the usage of CAD systems, which provide them with a more comprehensive understanding of both the abnormalities and a more precise means of categorizing them [10]. CAD systems are provided to support the detection of diagnostic errors, the reduction of false-negative findings, and the provision of a second opinion when analyzing medical pictures. Several studies have indicated that including a CAD system in the disease diagnosis may increase source file correctness by minimizing inconsistencies across observers [13]. Similarly, CAD systems: [14] initiate well-established methods of continuing to support treatment judgment like biopsy-specific suggestions; [15] aid in diagnostic checkups; [12] decrease the number of needless false-positive biopsy specimens and thoracotomies; [16,17] and can be used to distinguish respectively neoplastic and noncancerous tumors. Because of the success shown in clinical trials, CAD models are increasingly being utilized to detect lung cancer. If lung nodules can be detected at an early stage, adopting such systems may improve patients' chances of survival. To identify lung nodules, existing positron emission (CT) CAD applications seek breathing masses with certain physical properties (such as sphericity) [11]. So, studies are being conducted to see whether CT CAD can detect lung nodules. Early efforts to identify lung nodules relied mostly on non-machine learning-based approaches [18–24]. Later, the optimal border [31] was constructed using data-driven, machine-learning-based methodologies [25–30]. There have also been a lot of studies into deep learning (DL) techniques because of their predictive power. When compared to standard CAD systems, DL-based frameworks have the advantage of being readily optimized and applied for massive amounts of data [32]. DL, which is based on CNN's, has been a great assistance in the diagnosis and treatment of pulmonary nodules [33–36]. Finding the nodules, dissecting them, and classifying them are the three stages in DL's diagnostic process for pulmonary nodules. Locating the nodule falls within the purview of the detection method, while segmented tries to delineate the nodule's voxels and classification makes an educated guess as to the nodule's benign or malignant nature [31].

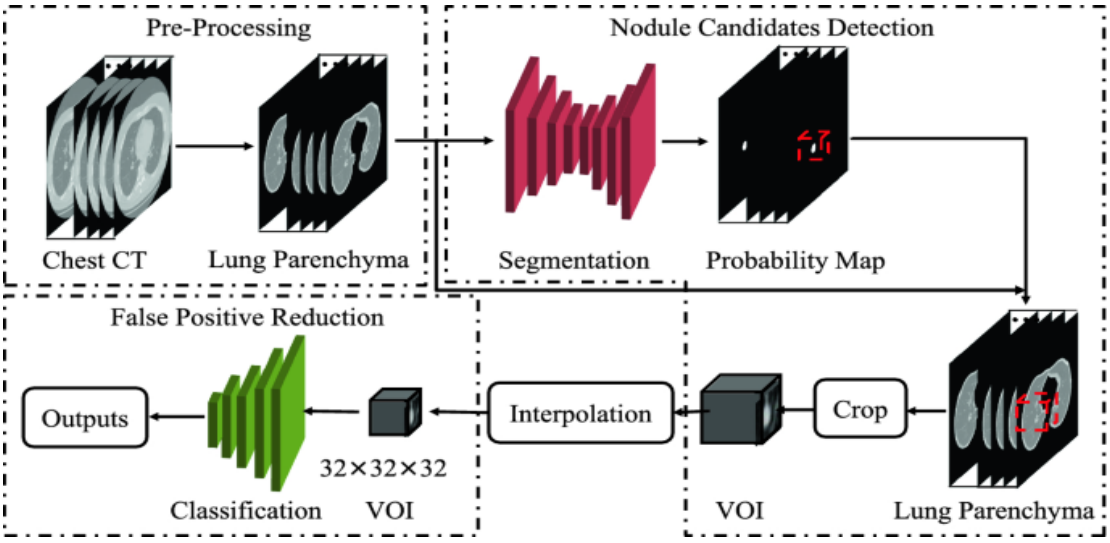

Fig. 1Visualization Effect of Lung Nodule

Prior study has examined the literature on pulmonary nodule detection [31, 32, 37–43] for several reasons. However, the focus of this research is on the lung CAD platform's better segmentation elements. When using a CAD system, it would be much simpler to determine if a suspicious area on the lung is indeed a nodule, whatever sort of nodule it is, and how large it is, because of the responsibilities of segmentation and classification. Furthermore, the literature on lung nodule segmentation is organized in this study based on a wide range of communication networks (broad sense neural net and Multiview CNN architecture). A novice in the area of research will benefit greatly from reading this since they will get insight into the proper methodology for doing future studies. The intended review research does this by discussing both newer and older works from reputable databases including IEEE Xplore, Web of Science, PubMed,

ScienceDirect, and Scopus that address the challenge of diagnosing lung nodules.

Because of this, the correct diagnosis is often delayed, and then when it is detected and verified, the disease has progressed to a later stage. Tests for conditions such as pneumonia, heart problems, and other lung issues may turn into lung cancer. However, only a few of them improve. Although researchers have been trying to develop an effective screening and treatment test for decades, it was not until recently that studies demonstrated that the findings of a low-dose computed tomography (LDCT) scan may help reduce the chance that dying from this illness. This article seems to be primarily concerned with segmenting CT-detectable lung nodules. The suggested method is developed and tested using a publicly available dataset. Recent articles that investigate this area of research often use Image Processing methods such as graph cuts [2], and fundamental Computer Vision centered on SVM[4], including hand-crafted features[20]. Users of this image processing technique may not have extensive background knowledge in the areas that benefit from the hand-crafted features. Features created manually are not only unreliable but also incompatible with the various CT scan types. Because data are not tagged, almost all existing approaches fail. Hand-crafted details are not conducive to a high-quality computer-aided diagnosis (CAD) system for detecting lung nodules. Successful picture classification was achieved using Convolutional Neural Networks (CNNs). Many modern neural network architectures have achieved accuracy levels that are comparable to or even beyond those of the ordinary person. That's an effort to find out where these connections can be utilized to locate the tiniest things that naked eyes would miss.

1.1. Broad CAD framework for detecting and diagnosing pulmonary nodules

Components of CAD systems vary widely. The most often seen components of a CAD system are data gathering, pre-processing, lung segmentation, lung nodule detection, false positive (FP) minimization, lung nodule edge detection, and lung nodule classification [42,44]. The pictures required by the CAD system are obtained at the processing stage of collecting data. CT is the best choice for somewhat early lymph node screening because of its excellent sensitivity and cheap cost [45]. In the first stage of processing, noise, clutter, and other distractions are removed. This improves the photos for the subsequent processing processes. CT scans are used in lung segmentation to delineate the lung from the neighboring thoracic tissue [46]. There is a two-stage process for treating FP: identification, where the lung tumor or movement is located, and then decrease. The slight error is significant since it requires distinguishing true lung nodules from false positives. The separation of computed tomography from lung parenchyma occurs during the segmentation stage. Next, in a process known as "feature extraction," the characteristics of the nodule are determined. These characteristics are then employed in the following stage when nodules are sorted into groups. Nodule classification, or identifying whether a nodule is benign or malignant, is the last and most crucial step in a CAD system. The Spatial Pyramid Pooling previous versions a pseudo-3D model that accounted for the sequential nature of the pulmonary slices.

2. Related Works

The first version of CNN was an enhancement of such an artificial neural network which employed convolutional operators to understand the challenges of the images it was given. Even though it was built on the same assumptions as the human visual system, it is very effective at solving pictures organizations find of any size. Each neuron's connections with certain other neurons allow it to process and react to sensory information. Each transmitter in a CNN only communicates with a small subset of "nearby" neurons, hence the network as a whole requires many fewer values than even a fully connected (FC) one. This is why CNN outperforms FC networks in image recognition and can be trained in a fraction of the time. Since its inception in 1996 [51], CNN has undergone significant changes to its network infrastructure. For instance, AlexNet [52] has 25 layers, VGG [53] has up to 152 layers upon layer, as well as ResNet [9] includes up to 1000 classes, all of which are correlated with improved performance.

Several techniques are developed to improve the accuracy of identifying lung nodule candidates in CT images by making use of deep learning's advantages. To distinguish between candidates with and without pulmonary nodules, Li et al. [55] presented a 2D deep learning model. The recommended network can be trained and evaluated using a dataset including 62,492 ROI image patches from 1,010 CT images from the LIDC/IDRI dataset. Forty-seven percent, or 20,772 patches, are nodules in the lungs. The remaining 21,720 fragments are benign. Testing shows that the approach can accurately diagnose lung nodules with a sensitivity of 89.0 percent and an accuracy of 86.4 percent.

Computer-assisted classification of lung cancer in CT images is an approach proposed by Kuruvilla and Gunavathi [56]. Mean, standard deviation, skewness, kurtosis, fifth centrally moment, and the sixth central moment was utilized by the authors to categorize the data. Evidence suggests that now the feed-forward backpropagation network outperforms the nutrient neural network in terms of classification accuracy. From our experimental results, we can conclude

that this approach has a 93.3% success rate, a 91.4% sensitivity, and 100% specificity. This demonstrates that the approach is effective in identifying noncancerous nodules.

When looking for pulmonary nodules, Choi and Choi [57] demonstrated how to apply hierarchical block categorization. To begin, the picture is discretely sectioned up into its constituent 3D planes. To locate possible nodules, the entropy evaluation is employed to choose informative blocks. Last but not least, a support vector machine (SVM) has now been conducted to analyze whether a given structure represents a nodule. According to the LIDC criteria, the method's accuracy is 97.2 %, its responsiveness is 95 percent, and its specificity is 96.2 percent.

To identify individuals who may develop lung nodules, Setio et al. [58] turned to Multiview convolutional networks (ConvNets). It was with 1,186 tumors first from LIDC/IDRI dataset that the LUNA16 challenge trained its approach. Evaluated results reveal a 90.1% improvement in sensitivity using this strategy. To identify promising nodule candidates, Torres et al. [14] used a feed-forward neural network (FFNN). There are 13 input neurons, 1 concealed neuron with 25 neurotransmitters, and 1 output neuron displaying the binary classifier in this network. Candidates were trained and evaluated using 1018 CT images from the LIDC/IDRI dataset. The test findings indicate responsiveness of up to 89.1 percent using this procedure.

It was proposed in the LUNA16 competition [59] that the LIDC-IDRI dataset [60], the biggest public benchmark collection of CT scans, may be used to evaluate completely automated nodule identification methods. Researchers were given 1,186 lung nodules based on CT scans obtained from the LIDC-IDRI. Competition findings reveal that the top individual detection system can currently identify pulmonary nodules with an accuracy of up to 92.9%.

2.1. Medical Image Analysis and Convolutional Neural Networks

The first time convolutional neural networks (CNNs) were used to analyze images was in AlexNet[5]. CNNs typically consist of four layers: the Convolutional Layer, the Pooling Layer, the Activation Layer, and indeed the Fully Connected Layer. Contrasted with natural pictures, medical images provide unique challenges for image analysis see figure 2. The databases are not only complex and difficult to grasp for non-experts, but they also pale in comparison to other activities' larger datasets.

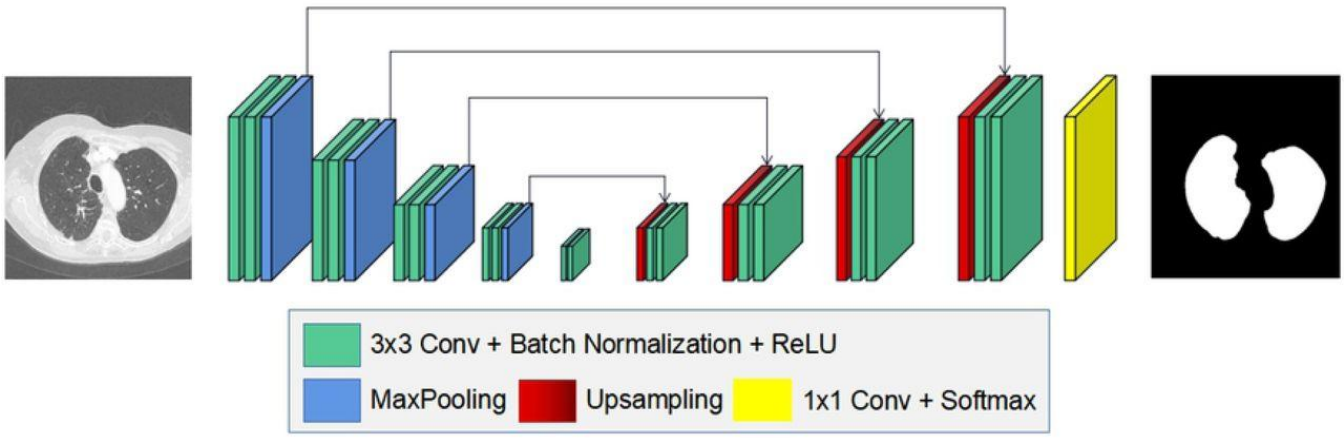

Fig. 23D CNN Architecture

2.2. U-Nets

U-Nets should be the pioneering effort in a new class of CNNs designed for this purpose. They have the same issues with tiny datasets and the necessity to localize areas instead of categorizing them [12]. Up appropriate sampling operators are used in place of pooling layers to expand a contracting network. This leads to improved output settling. Using the high-resolution characteristics from the shrinking route and the result of these up-sampled layers, a location may be determined. Significant improvements may be generated by using a convolution layer. Due to the abundance of feature channels, higher-resolution layers may be informed of the larger picture. Given that the expansion route is identical to the contracting path, as illustrated in Fig. 3, this results in a U-shaped network. There are no interconnected layers in this design. Most previous research on lung nodule segmentation relied on a hybrid network consisting of convolutional neural network (CNN) blocks and the more conventionally-styled fully-connected layers. U-Net but also Fully Convolutional Neural Networks are two common examples of these types of networks (FCN). Numerous research has shown the importance of convolutional CNN architecture in lung segmentation, particularly in segmentation systems like FCN and U-Net. The functions of these interconnected systems are dual. To begin, a down-sampling procedure is used to remove the

feature point maps while preserving the essential data. Second, "upsampling" is used to enlarge the feature maps to create a better-quality main picture.

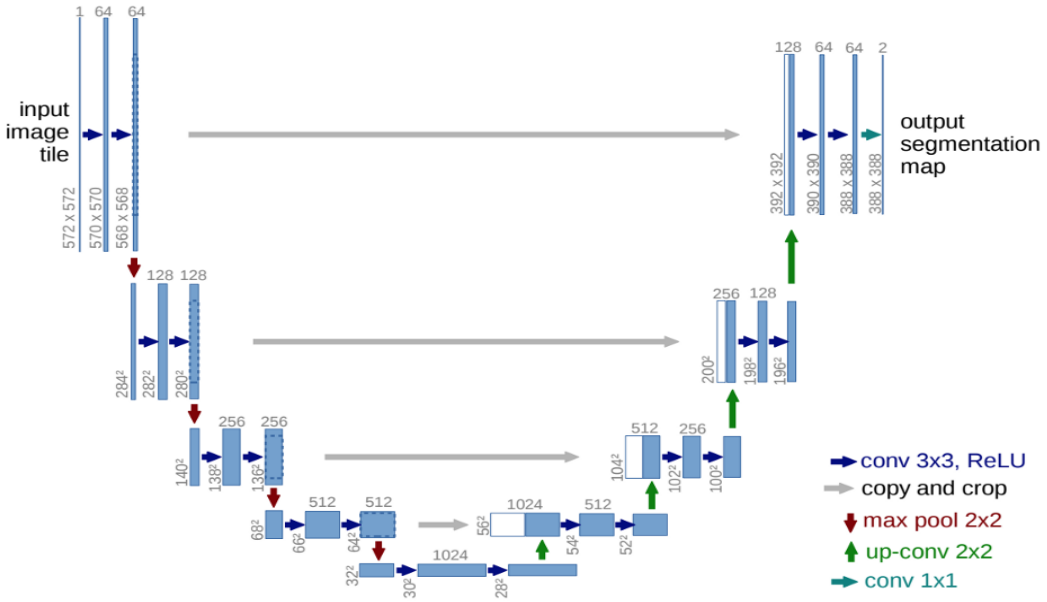

Fig. 3U – Net Architecture

3. Proposed Model

3.1. Datasets

Important for DL models are datasets. This is because better training datasets are employed to generate performance improvement of sophisticated learning algorithms. However, acquiring a large number of labelled training sets may be time-consuming and expensive. As a result, there is a dearth of publicly available datasets that may be used to further the development of lung nodule computer-aided diagnosis (CAD) systems. Public datasets have been built to facilitate research into the detection of lung nodules using CT, and although some organizations have made major contributions, this information lacks common measures for the protection of nodule characteristics and employs different labeling methodologies. Some records, for example, are labeled according to the parameters of the polygon's triangles, while others are labeled according to the form of the nodule's middle as well as radius. Several databases are used in the study of lung nodules, and brief descriptions of these resources are provided below. There are 1018 CT scans in DICOM format that have been tagged up with identifiable lesions and are available via the Lung Images Dataset Cooperative and Images Distributed Resource Initiative (LIDC-IDRI). Annotations for use in diagnostics are given in XML format. Each CT scan was annotated and corrected in two stages by a group of four highly experienced thoracic radiologists.

In the first step, radiologists looked at each CT scan independently and categorized the lesions as either "nodule 3 mm," "nodule = 3 mm," or "non-nodule 3 mm." After double-checking the corresponding labels on the other lesions, the radiologist with the most confidence in his or her diagnosis made the ultimate decision.

The extensive Tumor Segmentation Screening 16 (LUNA 16) collection was developed by LIDC-IDRI. Radiologists have annotated a total of 36,378 points on 888 select CT pictures. The authors only included annotations defined as nodules that were 3 mm or less; they did not consider nodules greater than 3 mm or non-nodule abnormalities. There were a total of 1186 nodules that were considered to be exceptional cases (i.e., the lesions that the algorithms should detect). Markings on sites with another nodule, i.e. those of various sizes, were just not recorded as false positives or true positives; rather, the irrelevant findings were eliminated from the evaluation.

The LIDC-IDRI is a resource for diagnosing and screening for lung cancer that includes computed tomography (CT) pictures of the chest with annotated lesions marked on them. In the first stage, the CT scans were evaluated by a panel of four radiologists, who divided the nodules into three categories depending on their size (3 mm, 3 mm, and 3 mm). The next step included each radiologist evaluating their annotations alongside those of the other three radiologists in an anonymous manner. From the larger LIDC dataset, we extracted a smaller dataset termed

LUNA16 consisting of 888 pictures; we did not include any scans with a slice thickness of more than 2.5 mm. The collection's metadata provides a variety of information about each image, including its geolocation and the spherical and quadratic measurements of the modular feature. The dataset is extremely varied, with scan thicknesses between 100 and 500 units. There are several benign and malignant tumors of differing degrees.

3.1.1. The subdivision of lung nodules

In the field of computer vision, segmentation is a technique used to divide a single image into many pieces (which can be 2-dimensional or 3-dimensional). The focus of this section is on simplifying the analysis of photographs so that not only experts but also the general public may benefit from the results. The process of segmentation is used to pick out certain elements in a picture, such as lines, corners, and edges. To be more specific, in the realm of three-dimensional data, every voxel in an image is labeled, and spatial information that shares this very same label is presumed and has the same properties. Therefore, either a set of shapes is recovered or a set of segments covering the whole image is constructed. The user specifies a region in which all the voxels share the same color, strength, or texture. There is a significant variation in the same traits across close geographic regions. These outlines may then be utilized to generate 3-D reconstructions with the help of various interpolation techniques like Marching Cubes. Using segmentation, we may more precisely identify the problem's origins. For a correct diagnosis, it is essential that radiologists carefully review segmented nodule imaging. In cases when the technology is only performing detection, such as the one described above, its attitudes or behaviorsare analogous to a black box where the user has no access to the underlying predictors. To address the complexity of the issue at hand, we may use the concept of partitioning. Patients and radiologists alike will benefit from this use of computer-aided design (CAD) technology.

3.2. Pre-processing

Multiple techniques are used to preprocess the LUNA16 3-D CT images. Photos in their present form are unsuitable for segmentation when they're too noisy and detailed. In the first step, the voxel data is converted into Houndsfield units (HU). The segmentation method and the Market-driven Watershed algorithm[11] are then used to isolate the lung tissue from the rest of the image while simultaneously filtering out background noise and potentially harmful substances like blood. As an example, lung tissue (with a HU concentration of around 500) is of primary importance. Air with a density of 1000 HU is pleasant in other places. Tissues like blood and water (which are about 0 HU) tend to mask the 700 HU of bone. Given that different CT scanners generate scans of varying intensities, a uniform result in terms of texture is not required.

It takes a lot of processing power to run 3-D convolutions on 3-D images using a 3-D architecture and 3-D filters. Training requires a GPU since the networks can be trained efficiently without one. It is impractical to use the dataset to train all at once due to connectivity challenges and time constraints. Because of this, training is carried out manually in batches using the transfer learning principle. Of the dataset's 1,000 pictures, 800 have been used for training and testing, leaving 88 for evaluation. The last group, out of a total of 88, has the fewest photos (89). Each subset is used independently during network training. We use a random seed to initialize the weights, and then when the whole subset has been returned, we modify and save the weights. When it comes to the other categories, the same protocol applies. Initial training is characterized by widespread overfitting, but as additional batches are added, the system architecture gradually improves, leading to more accurate data segmentation. PyTorch was used to train the network, while SimpleITK was used to show the segmentation results.

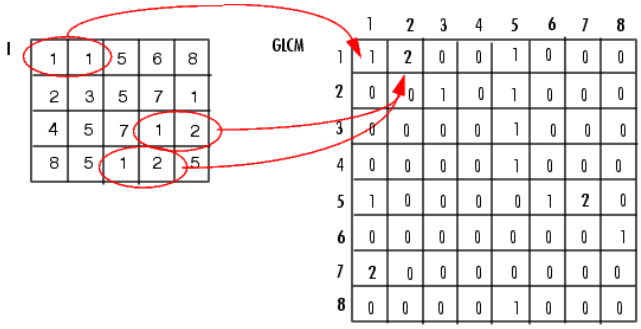

Fig. 4GLCM Matrix

3.3. Radiomics-Based Gray Level Co-Occurrence Matrix (GLCM)

We could use radionics to create a GLCM. The radionics research generates a gray level co-occurrence matrix by counting the number of times pixels with force (small level) respect I am spatially adjacent to pixels with value j. (GLCM). Conventionally, the spatial connection is shown by the on-focus picture and indeed the image to its centerfield (on the plane next to it), however, there are also other spatial links between the two pixels. Every chunk I j) inside the resulting glcm measures shown as figure 4, the number of times pixels occurred to me in the predefined spatial relationship with the image concerning j in the knowledge and perceived. Even though it would be impractical to plan and compute the GLCM for both the largest possible unique image size, RADIOMICS enlarges the data picture. Scaling is used by RADIOMICS, as normal, to decrease the monochromatic article's luminance from 256 to 8. The total number of drilling levels will establish the GLCM scale's precision. Control the overall radiance of the GLCM and the electric scaling by using the

RADIOMICs' numeric levels and gray limits. You may find more details in the RADIOMIC references section. The GLCM also suggests some concrete steps that might be taken to improve the situation. Check to see GLCM Capable of Deriving Metrics for more details.

3.4. Classification of lung nodules

The following is a synopsis of our training and evaluation methodology. In the first stage, we trained the model's image analysis stage for nodule recognition using images and radiologist comments from the LIDC/IDRI cohort. We also annotated more nodules from the publicized LUNA16 Challenge. The classification step of the model was then trained to predict the presence or absence of lung cancer in a CT image without the use of a priori nodule labeling. To translate this probability into a categorical label for training and validation, we choose a threshold of 0.5. The DSB2017 Competition's stage I CT data was used for training, and stage II CT data were used for validation. We utilized the regression coefficients classification from the DSB2017 tournament to train the classifications stage and save training time by minimizing log loss. This paper concludes with findings from generalization testing done on the approach and uses a selection of low-dose CT pictures from the NLST study.

3.5. Spatial Pyramid Pooling model

Spatial Pyramid Pooling is a method that uses many variables and a series of slices to determine whether or not a nodule is cancerous. The different-sized nodules are then detected using a spatial pyramid. Consecutive Information Extraction Across Slices Employing a Fake Three-Dimensional Model. CT scans were shown as three-dimensional volumes. For example, the typical resolution of a chest CT scan is around 512 by 512 by N, where N is the slice thickness. The internal and exterior resolutions of the 2-D slices may be different. Since a regular convolutional network can only process 2D input, the scan must be treated as N independent 512 x 512 slices.

Slice-based processing eliminates almost all dimensionality, making it impossible to recover relevant context. An artery in the body that runs perpendicular to the plane of the image in the z-dimension seems to be a small nodule when seen from an oblique angle. As can be seen, the 3-D input may be handled by a 3-D convolutional network, although such a network has its limitations. Compared to a 2-D model, training a 3-D CNN model is more difficult because of the larger number of parameters it uses.

It is common practice for training a 3D network to need a much larger training data set. Instead of a true 3D model, we settled on a pseudo-3D representation. Our technique takes advantage of the fact that an image may have several channels (typically three) and encodes neighboring slices as a variety of channels of a single image. See Figure 2 for a detailed explanation of how we use the slicing itself as one of the "green" channels while also adding a slice upward from the "blue" channels and a slice from underneath as the "red" stream, both at a distance of 4mm. Using multi-task learning, features are retrieved for classification techniques of the readily identifiable nodules. Segmentation networks can only provide a 2-dimensional shape for every nodule that is identified, and the shape boundary is often unclear due to low decision confidence. Several parameters may be extracted, including length, median certainty, and area ratio, but they fall short of capturing the characteristics of nodules that would be immediately apparent to a professional seeing the original volumetric image. The LIDC/IDRI collection contains around 1000 CT images with expert annotations. For each nodule, several descriptive features, including intricacy, homogeneity, lobulation, etc., are displayed in conjunction with the nodule outlines. Concurrently matching these 9 features: subtlety, sphericity, margin, lobulation, supposition, texturing, malignancy, calcification-1, and classification-2 required the development of a multi-task fully convolutional (see Figure5).

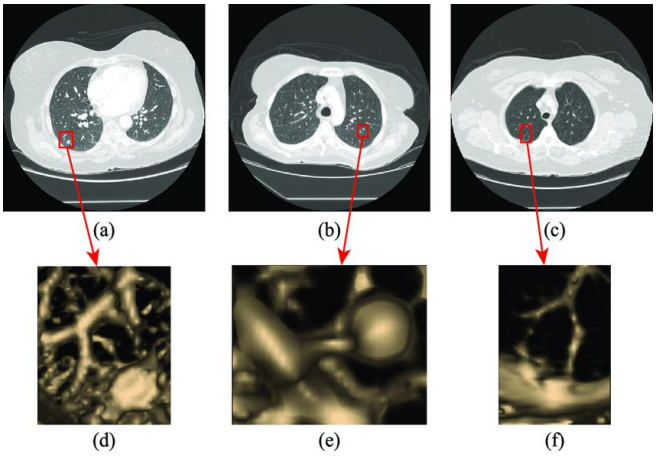

Fig. 5Lung Spatial Pyramid Pooling model

Some of LIDC/category IDRI's features were redundant, therefore we didn't use them all. We separated the category characteristic of "calcification" into two parts. The LIDC/IDRI annotations are used as the ground truth when training the extraction features network to ensure consistent numerical ratings across many properties. Gradient boosted trees may be the next computer module after the feature extraction network, and they are capable, known as gradient boosted trees (GBDT).

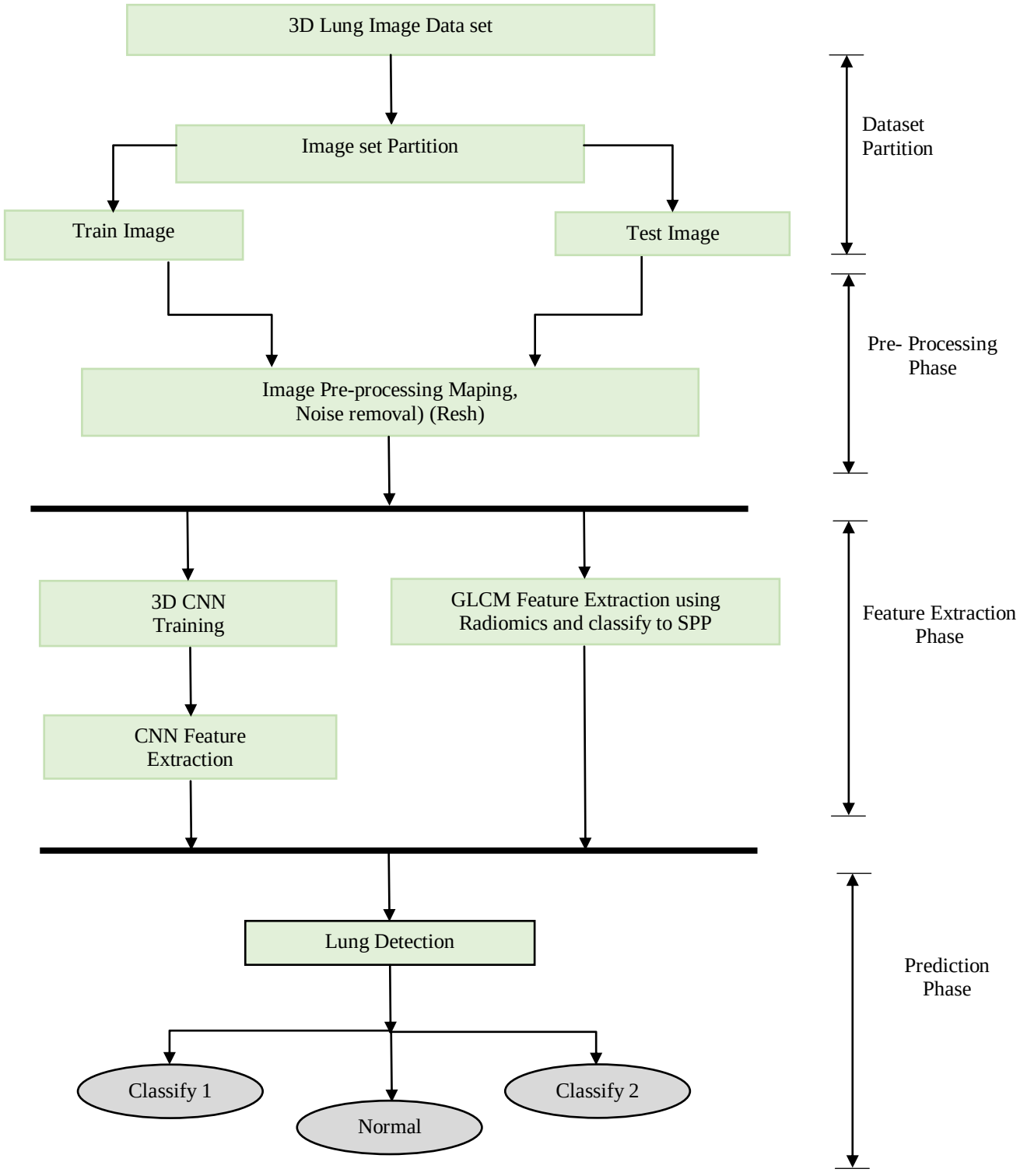

Fig. 6Proposed Flow Work

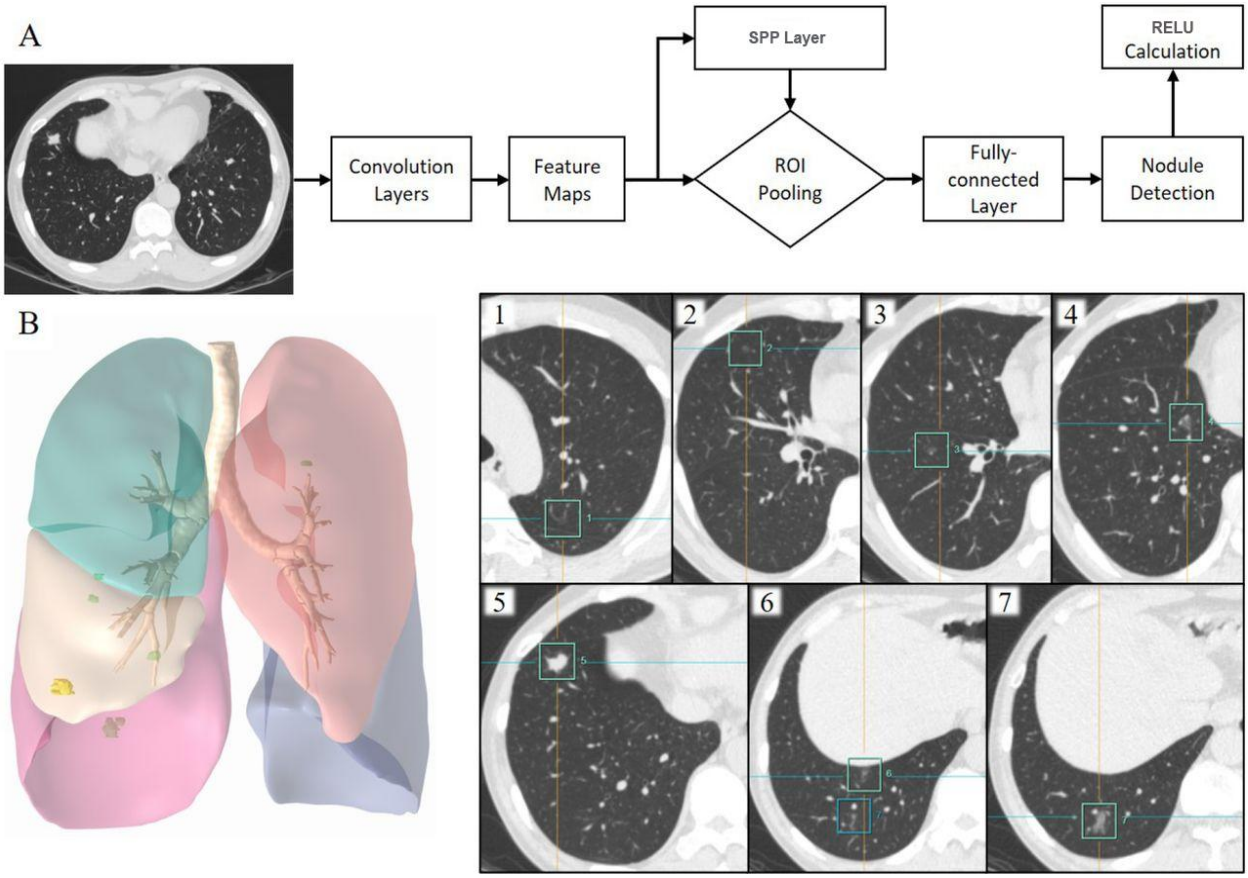

Fig. 7Proposed Classification Work

3.6. Using Spatial Pyramid and Feature Pooling to Detect Various Scales

After segmentation, nodule detection, and feature extraction, we were able to convert each CT volume into a table including nodule positions (x, y, z) and characteristics (size, subtlety, etc). To learn from this list using GBDT, we concatenated it into a vector with a fixed number of dimensions. The spatial pyramid methodology [19] was employed for the pooling. By segmenting the three-dimensional space in several ways, we were able to pin down the exact number of overlapping regions. Figure 4 illustrates two common types of partitions, each with four portions. Each region's feature vector was constructed using the features of the largest nodule in that region or was set to zero if no nodules were present. The feature maps from each region were combined to produce the extracted features that reflect the whole CT volume. Although the spatial pyramid depicted the whole of a CT scan, it may be used to accurately portray a single nodule by excluding other structures included in the image. By doing so, we may potentially assign a confidence score to each nodule using the GBDT classifier. The patient-level classifier takes this set of scores and uses it to produce a unique confidence interval in the region [0,1], which is also the threshold (set to 0.5 by default) to derive the unambiguous labels "cancer" or "no cancer." (See figure 6 and 7).

4. Research Methodology

In this study, we used V-Net (See figure 8), a three-dimensional CNN model optimized for prostatic CT volume segmentation. The prostate may take on a wide range of appearances throughout scans due to deformations and intensity fluctuations. Artifacts and distortions are produced as a result of spatial inhomogeneity in these photographs. Anatomical boundary estimate accuracy is therapeutically relevant during treatment. To achieve its distinctive impartiality, this design uses a training-optimized Dice correlation.

This model was built with medical image processing in mind, with unique tweaks to the channel's structure and hyper settings to ensure optimum available results could be reached in a feasible time. It uses a complete convolution layer, PReLu layers, and residue left to ensure that the

sophistication of the networks has no bearing on the convergence time, among other innovative characteristics. Bulk density kernel of size 5x5x5 voxels are employed in all convolution procedures at each level. A picture's resolution will decrease as it passes through the various compression phases. This is performed by performing compounding with filtering that are 2 voxels large on all flanks (a stride frequency of 2) towards the inputs. Next, we execute the extraction of features utilizing non-overlapping 2x2x2 volumetric patches, which provide extracted features with half the dimensions. Therefore, there is no need for any more pooling layers.

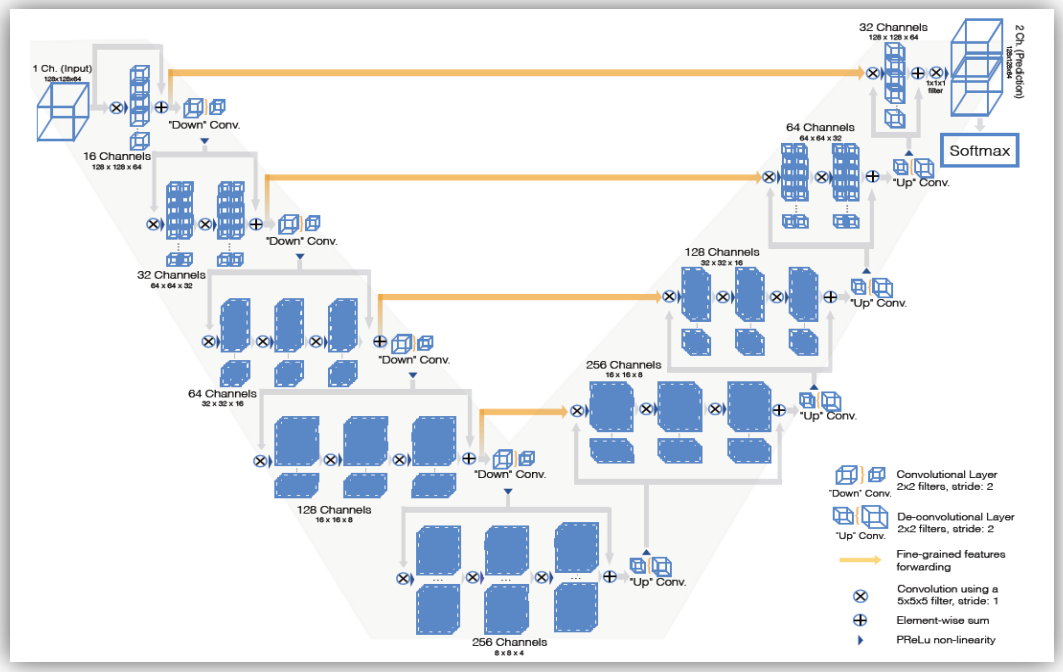

Fig. 8V- Net Architecture

They can indeed be considered to be effective forwarding causative agents of the elevations and up-gradation during stochastic gradient descent as the network goes deep. When it comes to effectively training CNN architectures and resolving challenges like the Dying ReLU, ReLU layers are notable ones that produce significantly better results than previous kernel functions like sigmoid, etc. Leaky ReLUs or Adaptive ReLU levels are two potential strategies to alleviate this problem. The recommended model takes more use of Leak ReLUs, whereby set the coefficient in the calculation $y = x$ to a value of 0.01 for negative numbers.

Upon that training dataset, PReLU seems to have the lowest error, while Leak ReLU and RReLU have mistaken that are greater than ReLU. It shows that PReLU might well have major overfitting concerns in small datasets.The notion of parameterized rectified linear According to the experts, it performs substantially better than ReLU in large-scale photo classification tasks. And that therefore it is trained using backpropagation, it is substantially like a leaking ReLU (Eqn. 1).

$$y_i = \begin{cases} x_i \\ x_{i/a_i} \end{cases} if_{x_i} < 0 \qquad (1)$$

Because no switches are required to transfer the pooled levels' output to their inputs, memory utilization during model training is reduced by using convolution operations instead of pooling operations. Specifically, this is seen in Fig. 3. By downsampling, the original signal's amplitude may be decreased while the characteristics derived in later layers can cover a larger area. In the model's left-hand portion, the number of features is shown to double between stages. To process the input data and provide the desired output, the relevant node in the network conducts extraction of features and spatially supporting augmentation of feature maps with varying resolutions. We get a volumetric segmentation at several outputs. Each voxel has an equal probability of belonging to the foreground (the nodule in this instance) or the background (the lungs), and the resultant output is two 3-dimensional volumes of the same size as the 3-dimensional image used as input.

CNN's arrows indicate that the show's elements progress to the right side of the screen after completing each stage on the left. Perfectly alright knowledge which would have been lost within the depths of the decompress pathway may be absorbed in this way, enhancing the quality attributes of the contour prediction. The deepest part of the CNN can record the whole input loudness. This characteristic is essential for segmenting anatomy that is not immediately visible, and it enables us to create a comprehensive solution when paired with the fine-grained information from the transmitted features.

$$D = \frac{2.\sum_i^N p_i g_i}{\sum_i^N p_i^2 + \sum_i^N g_i^2} \quad (2)$$

Dice coefficients are used to generate the objective function. If the preceding example is any indication, the optimal value for any quantity is somewhere between zero and one. The dice coefficient (also known as the overlap index) is the most often used performance measure for checking medical volume segmentation. It's a common tool for comparing synthetic segmentations to the raw data and measuring the reliability of the results.

4.1. Simplification

With so many more practice images available than is often the case in the medical field, we may forego any enhancements to these images. Spatial extrapolation using control points of PRELU is the most often used method for extending the LUNA and LIDC datasets. By comparing input and output, residual interconnections reveal the impact of intermediate layers on the model's learning ability.

4.2. Result Findings and Discussion

Our results showed a correlation of 0.98 on the testing data consisting of 88 LUNA16 photos of varying intensities and resolutions. The networks were sufficiently generic to properly detect and segregate the nodules across many CT scans. CNN's just recently being put to use in this field, but their promise is obvious. There were other images from the very same dataset that were utilized for testing but were hidden from the network input. The outcomes of the result in the different mapping (background and background) were mixed so that the nodule's context, or position concerning the lungs, could be examined and not lost.

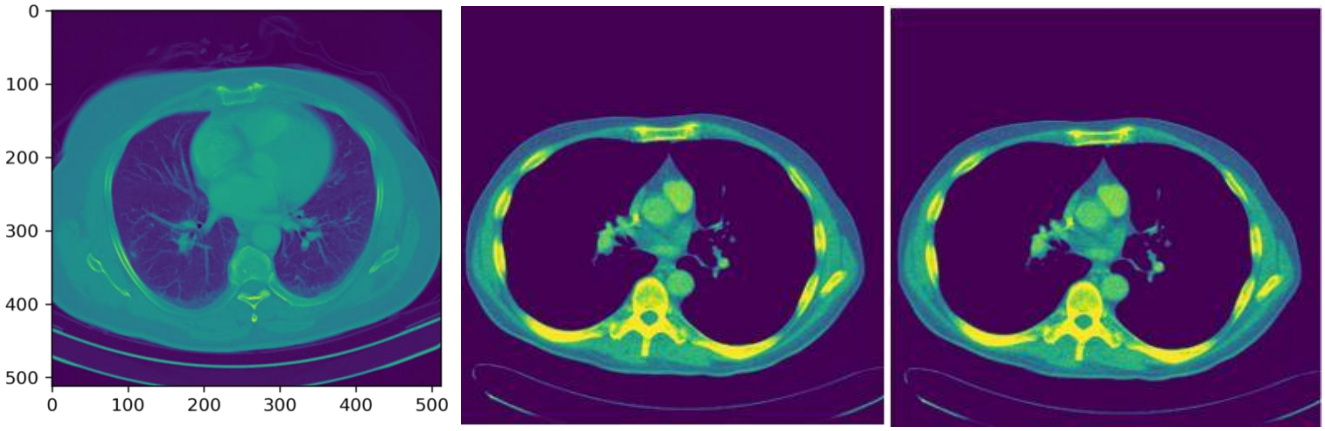

(a) **(b)** **(c)**

Fig. 9Pre-processing Image (a) Input Image. (b) Gaussian Filtered Image. (c) Localvar Filtered Image.

Table 1. Feature Extraction Parameter Value

Features	Values
Energy	2918821481.0
Entropy	4.920992838328338
Kurtosis	2.1807729393860265
Mean	825.235436306502
Skewness	0.27565085908587594
Contrast	74.04325876559685
Correlation	0.39322090748573196
Strength	0.9828367173152485

4.3. Project Flow Work

- **Step 1:** First Upload a real-time Lung Nodule dataset for lung-affected 3d CT Images
- **Step 2:** The dataset folder path to be created and added to Jupyter Notebook

- **Step 3:** The first stage is preprocessed model. We have a lot of dataset samples. In that, we use only one data to insert as input and then add the preprocess module, the module exact work from the 3D-CT image axis displayed via x, y, and z values. Then apply the resize () function, and the original image resize to 150*150*68.
- **Step 4:** Then the resized image is added to pepper and salt noise, the noise value is 0.05.
- **Step 5:** The Median filter technique to be applied for noise removal purposes
- **Step 6:** The noise is fully removed and converted to a binary image
- **Step 7:** 3D- CT Binary image converted to a grayscale image
- **Step 8:** In the Segmentation Process: the grayscale image is used to segment the stages and regions.
- **Step 9:** The image is separately divided into 3 axis - x, y, and z
- **Step 10:** The divided parts are accomplished by ROI Section. The ROI section illustrates the identified affected parts.
- **Step 11:** The exact identified affected region and histogram will be displayed at every stage Positive, Negative, and normal.
- **Step 12:** Then extract all features using the radionics GLCM technique,
- **Step 13:** The main theme is to Detect all stages using SPP and PRELU-based CNN-based algorithms to detect all stages.

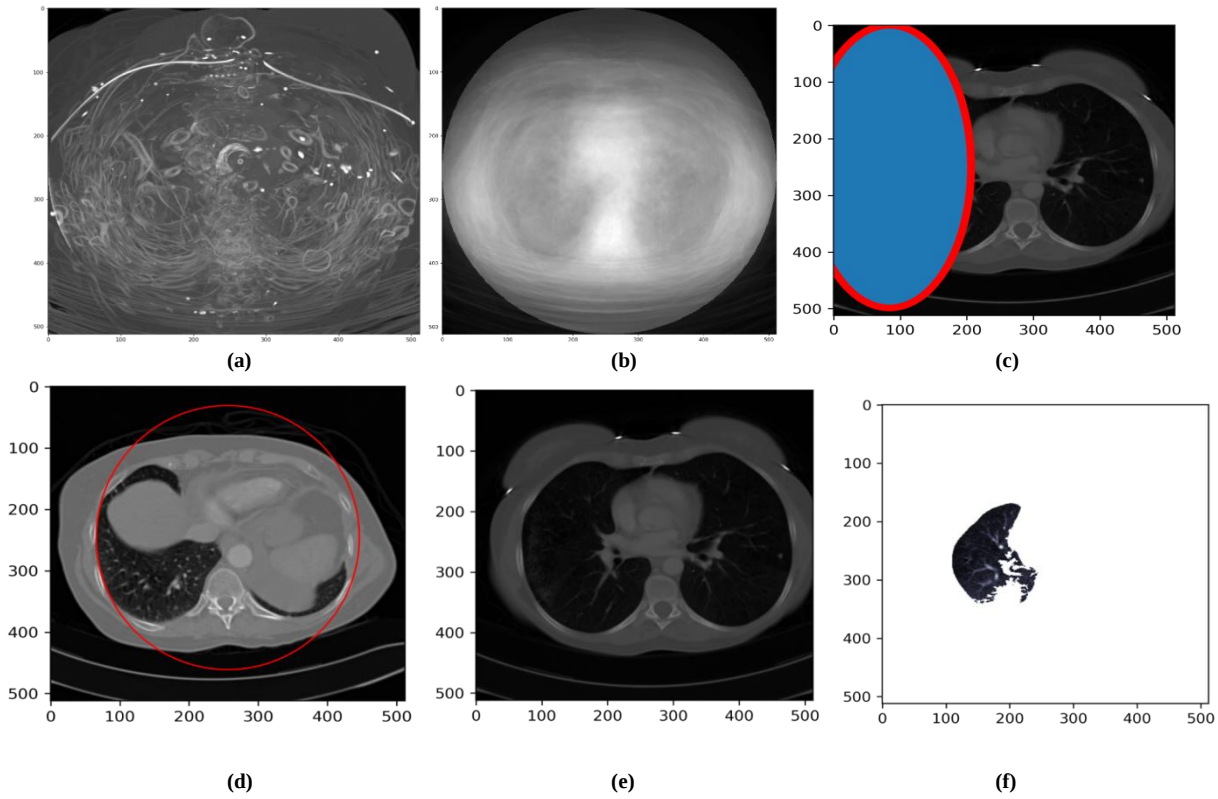

Fig. 10Segmentation Images. a) Fine Illustration of a Lung Infection. b) Surgical Resection of the Lung Image. c) Concealed Image Layering. d) Segmented Edge Image. e) Lung Mask Image. f) Lung Nodule Detection.

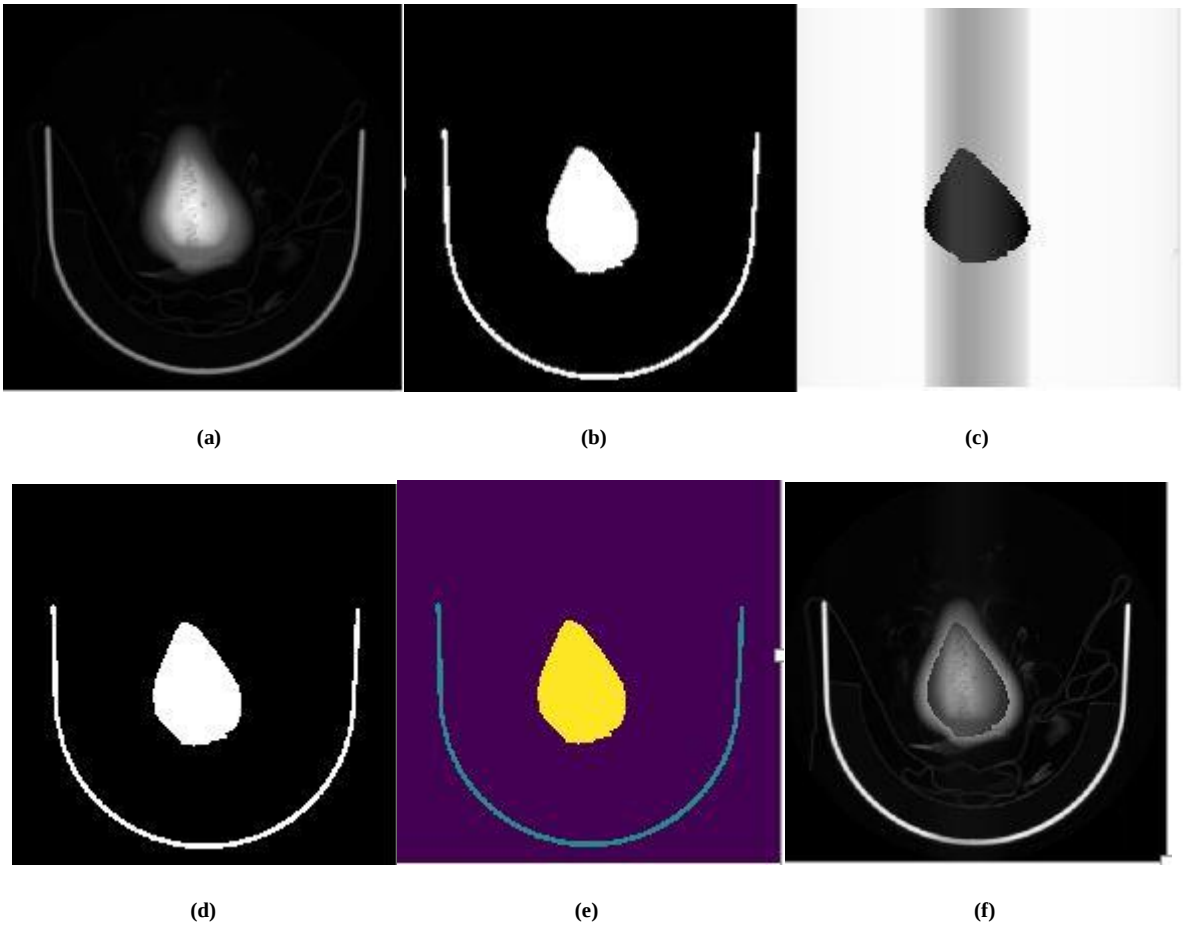

(a) **(b)** **(c)**

(d) **(e)** **(f)**

Fig. 11Framework of Detecting Steps for Mask Image. a) Original. b) Threshold. c) After Erosion and Dilation. d) Color Labels. e) Final Mask. f) Apply Mask on Original.

The aforementioned photos demonstrate that the model can handle several scan types. Even though CT scan quality varies depending on capturing equipment, the network is robust enough to appropriately separate them. There may be several nodules in a single lung. When there are several modules, the model can accurately separate them, resulting in separate divisions of all triple nodules. V-Net significantly outperformed conventional image processing techniques like watersheds and Markov random fields.

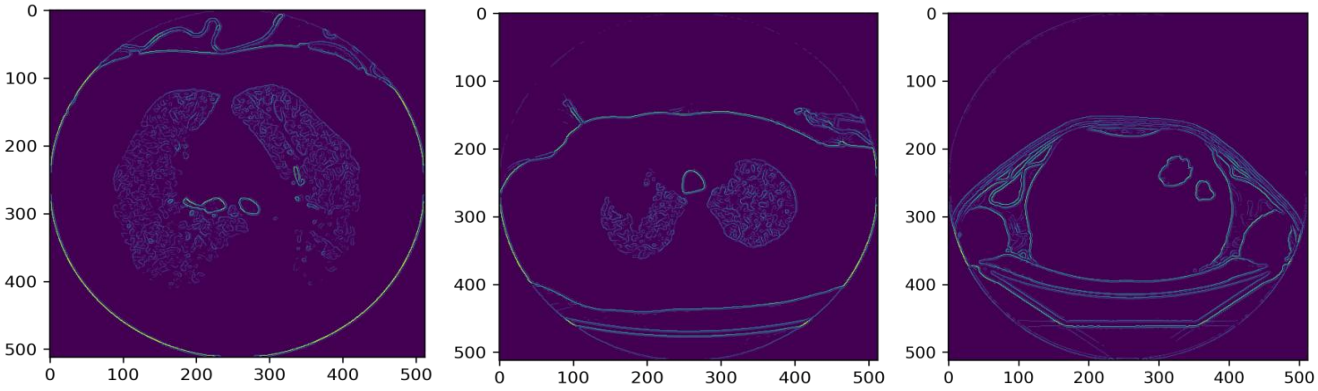

(a) **(b)** **(c)**

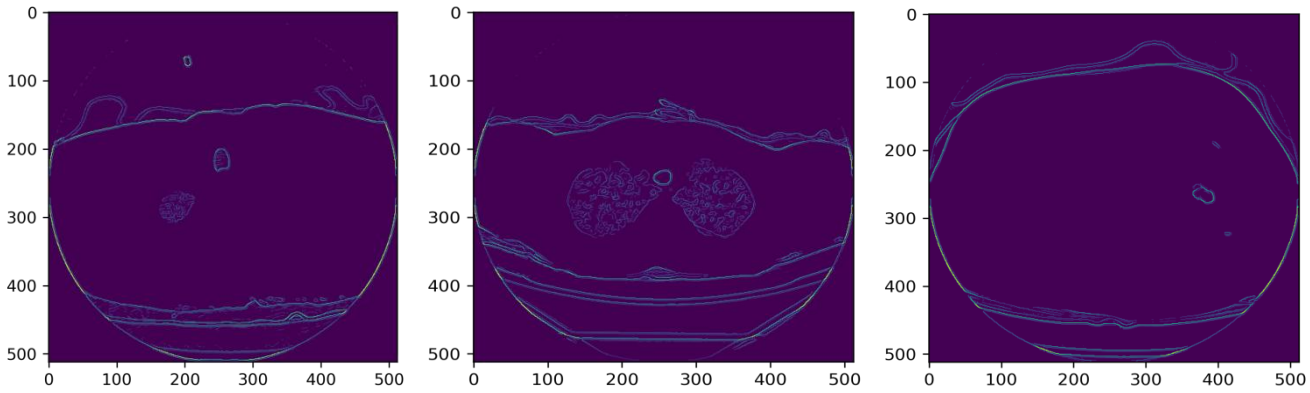

(d) **(e)** **(f)**

Fig. 12(a) – (f) Segmented Various Images

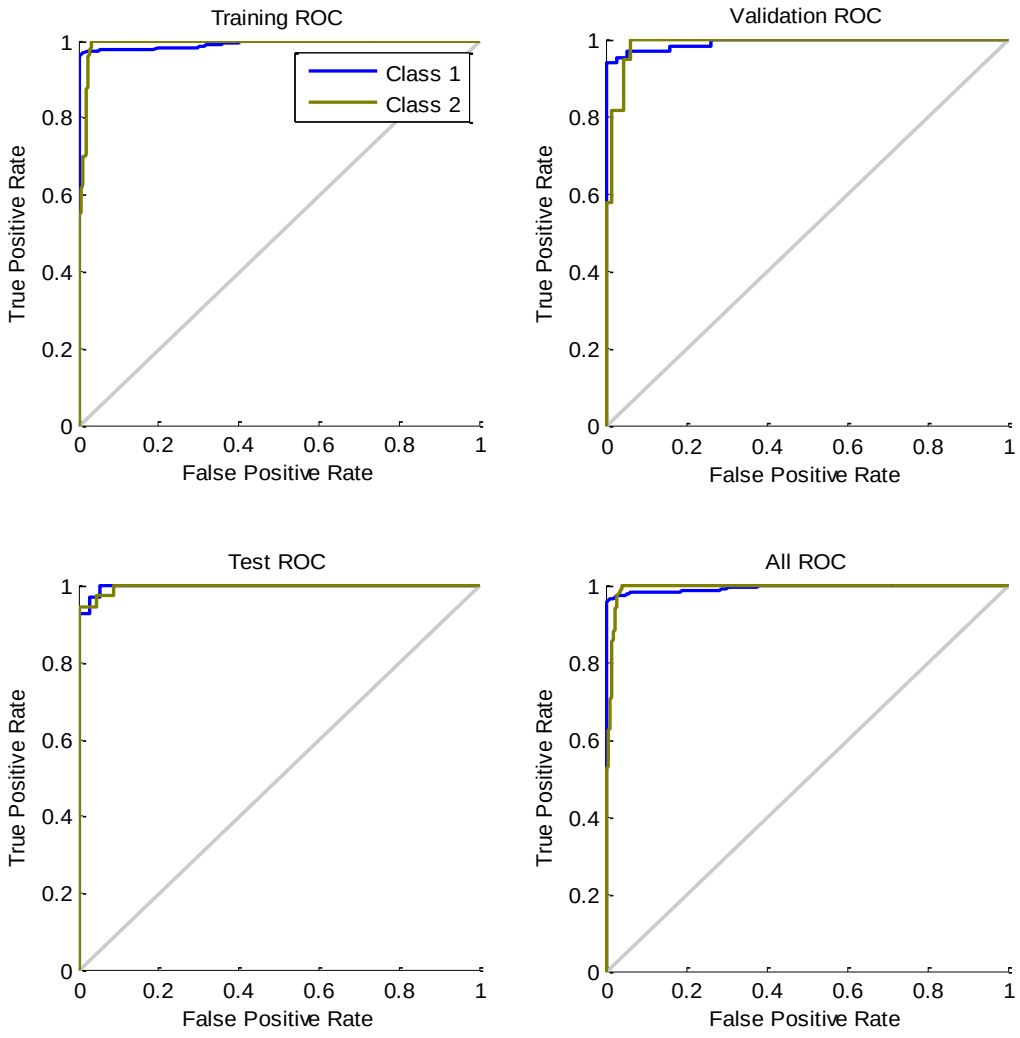

Fig. 13ROC for Training, Test, All, Validation

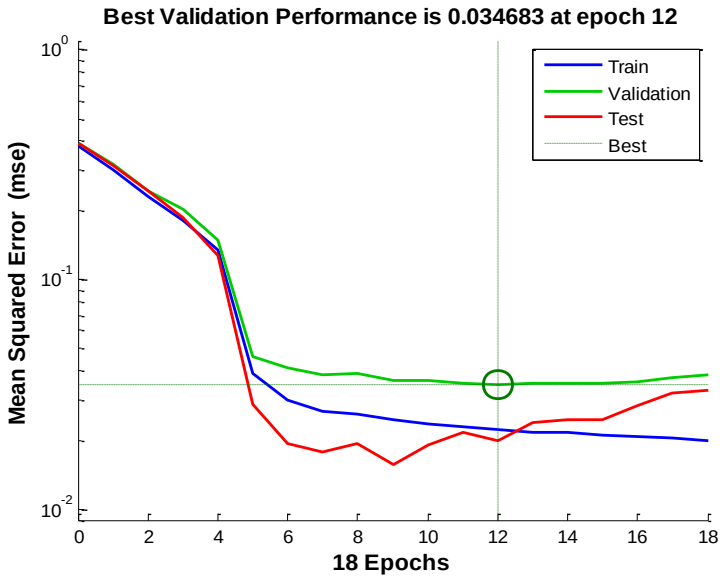

Fig. 14ROC for Training, Test, All, Validation

Table 2. Comparison Table

Classifier	Accuracy	Sensitivity	Specificity	AUC
Convolutional Neural Network **(X-Ray)**	92.00%	0.030	1	0.8
Convolutional Neural Network **(CT)**	97.10%	0.07	1	0.9

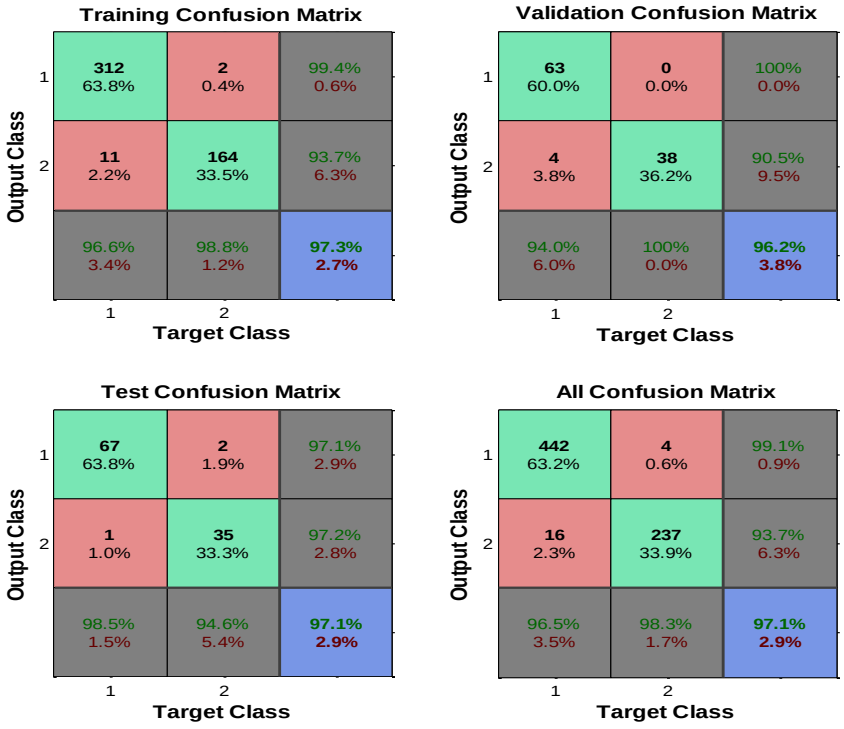

Fig. 15Confusion Matrix

With a sensitivity of 0.730 and a specificity of 0.998 for lung adaptability and a sensitivity of 0.730 and a specificity of 0.999 for illness, the models performed well. Above, you can see a table with further information on the hypothetical killing. This may be explained by the fact that a wide range of RELU layers, including PRELU and SSP, are actively pursuing grid combination morphology. Despite this, we were able to build a system that can separate a lung nodule with accuracy on par with that of models created on massive datasets using our medical image division technique. To evaluate the efficacy of our pipeline, we compared it to CT-scan-dependent nodule division approaches. The designers based their work on the 3D V-Net method. They could have been able to get a DSC of 0.6078 or 0.70355 for lung contamination. By employing our model, we were able to avoid this behavior. You should mention that we employed a pass dispersion of 80% preparation and 20% testing because although they used the modified appropriation (20 percent preparing and 80 percent testing). To address this problem, we developed a new neural architecture for creating polluted separation.

5. Conclusion

Recent studies using DL techniques have shown promising results for the detection of lung nodules in CT images. There is currently a lack of a reliable method for segmenting and classifying lung nodules for use in detection and diagnosis. Many lung nodule segmentation algorithms rely on generalized neural network architecture. Most research using neural networks included some innovative designs, such as collecting many photos of lung nodules and feeding them into the networks as inputs. In contrast, most of the general neural network-based methods were built on top of a V-Net architecture. Numerous lung nodule segmentation approaches were also employed to categorize the different lung nodule types, such as borders, layers, microscopic, well-circumscribed, and large nodules. A variety of classification schemes for lung nodules have been proposed (e.g., whether they are benign or malignant). Supervised learning, rather than semi-supervised learning, was used for the vast majority of the studies. Of the limited available data for training and validation of the models, LIDCIDRI is the most popular. Several tables summarizing the main findings were created to facilitate the comparison of the data from the different methods used. Several models used different criteria to verify their results across several datasets. Overall, the top-performing models vary greatly by data type, annotation needs, and research goals. Thus, it is not easy to judge how successful they are. Despite this limitation, our research shows that the need of developing trustworthy DL structures for accurately segmenting and categorizing lung nodules cannot be overstated. Finally, the emphasis of future studies should be on developing new suggestions and subscriber computer-based algorithms that may aid scientists and medical practitioners. In the future, it would be ideal if the model could be enhanced to have fewer false positives and to have visualization options that would help researchers and doctors better comprehend the machine's classification decisions. These adjustments are necessary before such instruments may be considered for inclusion in the standard set of diagnostic tools used in clinical practice.

Conflicts of Interest

Authors have no conflict of interest.

References

[1] A.A.Bankier, H.MacMahon, J.M.Goo, G. Rubin, C.M.Schaefer-Prokop, andD.Naidich, Recommendations for Measuring Pulmonary Nodules at CT: A Statement from the Fleischner Society, Radiology.285(2017) 584–600. [CrossRef] [PubMed]

[2] D.M.Hansell, A.A.Bankier, H.MacMahon, T.C.McLoud, N. L. Müller, and J. Remy, Fleischner Society: Glossary of Terms for Thoracic Imaging, Radiology.246 (2008) 697–722. [CrossRef] [PubMed]

[3] (2022) ELCAP Public Lung Image Database. [Online]. Available: http://www.via.cornell.edu/lungdb.html

[4] W.J.Choi, and T.S.Choi, Automated pulmonary nodule detection based on three-dimensional shape-based feature descriptor,Comput. Methods Programs Biomed.113(2014) 37–54. [CrossRef] [PubMed]

[5] P.Peloschek, J.Sailer, M. Weber, C. J. Herold, M. Prokop, and C. Schaefer-Prokop, Pulmonary Nodules: Sensitivity of Maximum Intensity Projection versus That of Volume Rendering of 3D Multidetector CT Data, Radiology.243 (2007) 561–569. [CrossRef] [PubMed]

[6] H.Kim, C.M.Park, J. M. Koh, S. M. Lee, and J. M. Goo, Pulmonary subsolid nodules: What radiologists need to know about the imaging features and management strategy,Diagn. Interv. Radiology. 20 (2013) 47–57. [CrossRef] [PubMed]

[7] (2022) Radiopedia, Pulmonary Nodule. 2020. [Online]. Available: https://radiopaedia.org/articles/pulmonary-nodule-1

[8] M.P.Revel, A. Bissery, M. Bienvenu, L.Aycard, C. Lefort,and G. Frija, Are two-dimensional CT measurements of small noncalcified

pulmonary nodules reliable?, Radiology.231 (2004) 453–458. [CrossRef]

[9] D.Han, M.A.Heuvelmans, M. Oudkerk, Volume versus diameter assessment of small pulmonary nodules in CT lung cancer screening, Transl. Lung Cancer Res. 6 (2017). [CrossRef]

[10] C.I.Henschke, D.I.McCauley, D.F.Yankelevitz, D.P.Naidich, G. McGuinness, O. S. Miettinen, D. M. Libby, M. W.Pasmantier, J. Koizumi, and N. K. Altorki, Early Lung Cancer Action Project: Overall design and findings from baseline screening, Lancet.354 (1999) 99–105. [CrossRef]

[11] R.A.Castellino, Computer-aided detection (CAD): An overview, Cancer Imaging. 5(2005) 17–19. [CrossRef]

[12] M.B.McCarville,H.M. Lederman, V.M.Santana, N. C. Daw, S.J.Shochat, C. S. Li, and R. A. Kaufman, Distinguishing benign from malignant pulmonary nodules with helical chest CT in children with malignant solid tumors, Radiology.239 (2006) 514–520. [CrossRef]

[13] S. Singh, J. Maxwell, J. A. Baker, J. L. Nicholas, andJ. Y. Lo, Computer-aided Classification of Breast Masses: Performance andInterobserver Variability of Expert Radiologists versus Residents. Radiology.258 (2011) 73–80. [CrossRef] [PubMed]

[14] M. L. Giger, N. Karssemeijer, and J. A. Schnabel, Breast image analysis for risk assessment, detection, diagnosis, and treatment of cancer, Annu. Rev. Biomed. Eng. 15 (2013) 327–357. [CrossRef] [PubMed]

[15] S.Joo, Y. S. Yang, W. K. Moon, and H. C. Kim, Computer-aided diagnosis of solid breast nodules: Use of an artificial neural networkbased on multiple sonographic features, IEEE Trans. Med. Imaging.23 (2004) 1292–1300. [CrossRef]

[16] T. W. Way, B. Sahiner, H. P. Chan, L. Hadjiiski, P. N. Cascade, A. Chughtai, N. Bogot, and E.Kazerooni, Computer-aided diagnosisof pulmonary nodules on CT scans: Improvement of classification performance with nodule surface features, Med. Phys. 36 (2009) 3086–3098. [CrossRef]

[17] T.W.Way, L. M. Hadjiiski, B. Sahiner, H. P. Chan, P. N. Cascade, E. A.Kazerooni, C. Zhou, and N.Bogot,Computer-aided diagnosisof pulmonary nodules on CT scans: Segmentation and classification using 3D active contours, Med. Phys. 33 (2006) 2323–2337. [CrossRef] [PubMed]

[18] M.L.Giger, N. Ahn, K. Doi, H. MacMahon, and C. E. Metz, Computerized detection of pulmonary nodules in digital chest images: Use of morphological filters in reducing false-positive detections, Med. Phys.17(1990) 861–865. [CrossRef]

[19] W. Ying, C. Cunxi, J. Tong, X. Xinhe, Segmentation of regions of interest in lung CT images based on 2-D OTSU optimized by genetic algorithm,in Proceedings of the 2009 Chinese Control and Decision Conference, Guilin, China.(2009) 5185–5189.

[20] R. Helen, N. Kamaraj, K. Selvi, and V. R. Raman, Segmentation of pulmonary parenchyma in CT lung images based on 2D Otsu optimized by PSO,in Proceedings of the International Conference on Emerging Trends in Electrical and Computer Technology, Nagercoil, India.(2011) 536–541.

[21] Y. Liu, Z. Wang, M. Guo, and P. Li, Hidden conditional random field for lung nodule detection, in Proceedings of the 2014 IEEE International Conference on Image Processing (ICIP), Paris, France. 3518–3521.

[22] J. John, andM. Mini, Multilevel Thresholding Based Segmentation and Feature Extraction for Pulmonary Nodule Detection, Procedia Technol. 24 (2016) 957–963. [CrossRef]

[23] A. Teramoto, H. Fujita, O. Yamamuro, and T. Tamaki, Automated detection of pulmonary nodules in PET/CT images: Ensemble false-positive reduction using a convolutional neural network technique, Med. Phys.43(2016) 2821–2827. [CrossRef] [PubMed]

[24] R. Mastouri, H. Neji, S. Hantous-Zannad, and N. Khlifa, A morphological operation-based approach for Sub-pleural lung nodule detection from CT images,in Proceedings of the 2018 IEEE 4th Middle East Conference on Biomedical Engineering (MECBME), Tunis, Tunisia.(2018) 84–89.

[25] A. M. Santos, A.O.D.C.Filho, A. C. Silva, A.C. de Paiva, R. A. Nunes, and M.Gattass, Automatic detection of small lung nodules in 3D CT data using Gaussian mixture models, Tsallis entropy and SVM. Eng. Appl. Artif. Intell. 36 (2014) 27–39. [CrossRef]

[26] H. M. Orozco, O. O. V. Villegas, V. G. C. Sánchez, H. D. J. O. Domínguez, and M. D. J. N. Alfaro, Automated system for lung

nodules classification based on wavelet feature descriptor and support vector machine. Biomed. Eng. 14 (9) (2015). [CrossRef]

[27] L. Lu, Y. Tan, L. H. Schwartz, and B. Zhao, Hybrid detection of lung nodules on CT scan images, Med. Phys.42(2015) 5042–5054.[CrossRef] [PubMed]

[28] F.V.Farahani, A. Ahmadi, and M. F. Zarandi, Lung nodule diagnosis from CT images based on ensemble learning,in Proceedings of the 2015 IEEE Conference on Computational Intelligence in Bioinformatics and Computational Biology (CIBCB), Niagara Falls, ON, Canada.(2015) 1–7.

[29] J. Klik MA, E. M. v Rikxoort, J. F. Peters, H. A.Gietema, M. Prokop, andB. v Ginneken, Improved classification of pulmonary nodules by automated detection of benign subpleural lymph nodes, in Proceedings of the 3rd IEEE International Symposium on Biomedical Imaging: Nano to Macro IEEE: Arlington, VA, USA.(2006) 494–497.

[30] B. R. Froz, A.O.D.C. Filho, A. C. Silva, A. Paiva, R. A. Nunes, andM. Gattass, Lung nodule classification using artificial crawlers,directional texture, and support vector machine, Expert Syst. Appl. 69 (2017) 176–188. [CrossRef]

[31] J. Wu, and T. Qian, A survey of pulmonary nodule detection, segmentation, and classification in computed tomography with deep learning techniques. J. Med. Artif. Intell. 2 (2019) 1–12. [CrossRef]

[32] K. Liu, Q. Li, J. Ma, Z. Zhou, M. Sun, Y. Deng, W. Tu, Y. Wang, L. Fan, andS. Liu, Evaluating a fully automated pulmonary nodule detection approach and its impact on radiologist performance,Radiol. Artif. Intell.1 (2019). [CrossRef]

[33] W. Shen, M. Zhou, F. Yang, C. Yang, and J. Tian, Multiscale convolutional neural networks for lung nodule classification, in Proceedings of the International Conference on Information Processing in Medical Imaging, Springer: Cham, Switzerland, (2015) 588–599.

[34] F. Ciompi, K. Chung, S. J. Van Riel, A. A. A.Setio, P. K. Gerke, and C. Jacobs, Towards automatic pulmonary nodule management in lung cancer screening with deep learning, Sci. Rep. 7 (2017). [CrossRef] [PubMed]

[35] J. Causey, J. Zhang, S. Ma, B. Jiang, J. A. Qualls, D. G.Politte, F. W. Prior, S. Zhang, and X. Huang, Highly accurate model for prediction of lung nodule malignancy with CT scans. Sci. Rep. 8 (2018) 9286. [CrossRef]

[36] K. L. Hua, C. H. Hsu, S. C. Hidayati, W. H. Cheng, andY. J. Chen, Computer-aided classification of lung nodules on computedtomography images via deep learning technique,OncoTargetsTher. 8(2015) 2015–2022.

[37] A.K.Dhara, S. Mukhopadhyay, and N. Khandelwal, Computer-aided detection and analysis of pulmonary nodule from CT images: A survey, IETE Tech. Rev. 29 (2012). [CrossRef]

[38] I. Sluimer, A. Schilham, M. Prokop, and B. Van Ginneken, Computer analysis of computed tomography scans of the lung: A survey, IEEE Trans. Med. Imaging.25 (2006) 385–405. [CrossRef] [PubMed]

[39] I.R.S.Valente, P. C. Cortez, E. C. Neto, J. M. Soares, V.H.C.Albuquerque, and J. M. R. Tavares, Automatic 3D pulmonary nodule detection in CT images: A survey. Comput. Methods Programs Biomed. 124 (2015) 91–107. [CrossRef]

[40] A. Halder, D. Dey, and A. K. Sadhu, Lung Nodule Detection from Feature Engineering to Deep Learning in Thoracic CT Images: A Comprehensive Review, J. Digit. Imaging.33 (2020) 655–677. [CrossRef] [PubMed]

[41] G. Zhang, S. Jiang, Z. Yang, L. Gong, X. Ma, Z. Zhou, C. Bao, and Q. Liu,Automatic nodule detection for lung cancer in CT images: A review,Comput. Biol. Med. 103 (2018) 287–300. [CrossRef]

[42] Y.Gu, J. Chi, J. Liu, L. Yang, B. Zhang, D. Yu, Y. Zhao, and X. Lu, A survey of computer-aided diagnosis of lung nodules from CT scans using deep learning,Comput. Biol. Med. 137 (2021) 104806. [CrossRef] [PubMed]

[43] Monkam, P. Qi, S. Ma, H. Gao, W. Yao, and Y. Qian,Detection and classification of pulmonary nodules using convolutional neural networks: A survey, IEEE Access.7 (2019) 78075–78091. [CrossRef]

[44] S.A.El-Regaily, M. A. Salem, M. Aziz, and A. Roushdy, M.I. Lung nodule segmentation, and detection in computed tomography, in Proceedings of the 2017 Eighth International Conference on Intelligent Computing and Information Systems (ICICIS), Cairo, Egypt, (2017) 72–78.

[45] E.E.Nithila, and S. S. Kumar, Segmentation of lung nodule in CT data using active contour model and Fuzzy C-mean clustering, Alex. Eng. J. 55 (2016) 2583–2588. [CrossRef]

[46] A. Mansoor, U. Bagci, B. Foster, Z. Xu, G. Z. Papadakis, L. R. Folio, J. K. Udupa, andD. J. Mollura, Segmentation and Image Analysis of Abnormal Lungs at CT: Current Approaches, Challenges, and Future Trends, RadioGraphics. 35 (2015) 1056–1076. [CrossRef] [PubMed]

[47] J. Zhang, Y. Xia, H. Cui, and Y. Zhang, Pulmonary nodule detection in medical images: A survey, Biomed. Signal Process Control.43 (2018) 138–147. [CrossRef]

[48] S. G. Armato, G. McLennan, L. Bidaut, M. F. McNitt-Gray, A. P. Reeves, D. R.Aberle, B. Zhao, andC. I.Henschke, The lung image database consortium (LIDC) and image database resource initiative (IDRI): A completed reference database of lung nodules on CT scans. Med. Phys. 38 (2011) 915–931. [CrossRef] [PubMed]

[49] A. A.Setio, A. Traverso, A. De Bel, T. Berens, M.S. Van Den Bogaard, and C. Cerello, Validation, comparison, and combination of algorithms for automatic detection of pulmonary nodules in computed tomography images: The LUNA16 challenge, Med. Image Anal. 42 (2017) 1–13. [CrossRef]

[50] K. Zarogoulidis, P. Zarogoulidis, K. Darwiche, E. Boutsikou, N.Machairiotis, and K. Tsakiridis, Treatment of non-small cell lung cancer (NSCLC). J. Thorac. Dis. 5 (2013). [PubMed]

[51] Y. Lecun, L. Bottou, Y. Bengio, and P. Haffner, Gradient-based learning applied to document recognition, in Proceedings of the IEEE, 86 (11)(1998) 2278–2324.

[52] A. Krizhevsky, I. Sutskever, and G. E. Hinton, ImageNetclassification with deep convolutional neural networks, inProceedings of the 25th International Conference on Neural Information Processing Systems. Curran Associates Inc., Lake Tahoe, NV, USA.1 (2012) 1097–1105.

[53] K. Simonyan and A. Zisserman, Very deep convolutionalnetworks for large-scale image recognition, in Proceedings ofIEEE International Conference on Learning Representations,Banff, AB, Canada.(2014).

[54] K. He, X. Zhang, S. Ren, and J. Sun, Deep residual learningfor image recognition, in Proceedings of 2016 IEEE Conference on Computer Vision and Pattern Recognition (CVPR),Las Vegas, NV, USA. (2016) 770–778.

[55] W. Li, P. Cao, D. Zhao, and J. Wang, Pulmonary noduleclassification with deep convolutional neural networks on computed tomography images, Computational and MathematicalMethods in Medicine.(2016).

[56] J. Kuruvilla and K. Gunavathi, Lung cancer classificationusing neural networks for CTimages, Computer Methods andPrograms in Biomedicine. 113 (1)(2014) 202–209.

[57] W.J. Choi and T.S. Choi, Automated pulmonary noduledetection system in computed tomography images: a hierarchical block classification approach, Entropy. 15 (2)(2013) 507–523.

[58] A. A. A. Setio, F. Ciompi, and G. Litjens, Pulmonary noduledetection in CT images: false positive reduction using multi-view convolutional networks, IEEE Transactions on MedicalImaging. 35 (5) (2016) 1160–1169.

[59] E. L. Torres, E. Fiorina, andF. Pennazio, Large scale validation of the M5L lung CAD on heterogeneous CT datasets,Medical Physics. 42 (4)(2015)1477–1489.

[60] A. A. A. Setio, A. Traverso, and T. de Bel, Validation, comparison, and combination of algorithms for automatic detection of pulmonary nodules in computed tomography images: the LUNA16 challenge, Medical Image Analysis. 42 (2017) 1–13.